

**NPL REPORT TQE 31**

**PROJECT REPORT ON 'METROLOGY NEEDS FOR QUANTUM  
COMMUNICATION NETWORKS'**

**FERGUSON, R. A, FELIX, J, TSE, A.**

**MARCH 2024**



Project Report on 'Metrology needs for quantum communication  
networks'

Ferguson, R. A, Felix, J, Tse, A.  
Electromagnetic & Electrochemical Technologies

© NPL Management Limited, 2024

ISSN: 1754-2995

<https://doi.org/10.47120/npl.TQE31>

National Physical Laboratory  
Hampton Road, Teddington, Middlesex, TW11 0LW

Extracts from this report may be reproduced provided the source is acknowledged  
and the extract is not taken out of context.

Approved on behalf of NPLML by  
John Howes, ELECMEAS Group Leader



## CONTENTS

<b>1</b>	<b>Aims/NPL, customer and industry need .....</b>	<b>1</b>
<b>2</b>	<b>Work package overview – ‘metrology needs for quantum communication networks’ .....</b>	<b>4</b>
<b>3</b>	<b>Insertion loss measurements on qu grade patchcords .....</b>	<b>6</b>
3.1	Commercial criteria. ....	6
3.2	System build.....	6
3.3	Software and testing .....	8
3.4	Measurements .....	10
3.5	Results. ....	12
3.6	Treatment of uncertainites .....	14
3.7	Linearity. ....	16
3.8	Summary .....	18
<b>4</b>	<b>Mode field diameter measurements on qu grade patchcords.....</b>	<b>20</b>
4.1	Commercial criteria. ....	20
4.2	Far-field system overview .....	22
4.3	Modifications .....	25
4.4	Measurements .....	27
4.5	Results. ....	28
4.6	Conclusions .....	30
4.7	Uncertainty contributions.....	32
4.8	Summary.....	34
<b>5</b>	<b>Concluding remarks and future collaborative opportunities .....</b>	<b>35</b>
	<b>Appendix 1 - example of a Senko specification sheet for a quantum Grade fc/upc patchcord .....</b>	<b>38</b>
	<b>References.....</b>	<b>39</b>



## 1 Aims/NPL, customer and industry need

The broad aim behind this project is to provide metrology for new high performance quantum grade interconnects, with traceable verification, used for communication links to create versatile and easy-to-use building blocks for distributing entanglement over fibre networks. These building blocks can be used to build a ‘Quantum Internet’ to enable applications such as ultra-secure communication and distributed quantum computing in hyperscale data centres, high performance computing (HPC) and 5G environments. The ‘building blocks’ primarily referred to in this report relate to the interconnecting conduits to transfer and distribute entangled photons, such as Quantum grade optical fibre patchcords as well as the optical fibre itself.

Single photons or entangled photons can be used to create extremely secure communication links or form an integral part of a quantum computer or measurement network. For this to work entangled photons need to be able to be sent over optical networks without “decoherence”, the collapse of the wave-function. Decoherence is caused by irreversible interaction between an entangled system and its environment and there is a clear risk of this as the photons propagate through an optical cable. These interactions can take the form of general scattering loss mechanisms such as, spontaneous Raman scattering, four-wave mixing, and amplified spontaneous emission, these are all major practical limiting factors for Quantum Key Distribution (QKD) and to future quantum networks [1].

QKD is also subject to a rate–distance limit, which defines the maximum possible secret key rate that two parties can exchange at a given distance using QKD [2]. This emerging field is therefore expected to fuel demand for a new generation of “quantum grade” optical cables and connectors. These low loss connectors will allow larger proportions of entangled photons to successfully propagate through optical networks without decoherence. This would increase the rate-distance limit of QKD and, improve the efficiency of the quantum optical network.

The range of interconnects utilised within any Quantum Internet or entanglement distribution system must possess extremely high propagating signal efficiencies. The inevitable inclusion of connectorized links, within a network, will potentially add to the loss budgets drastically reducing operating ranges. Knowledge of key parameters such as the insertion loss and mode field diameter (MFD) of these links and components are vital to maintain performance.

The insertion losses of commercial links within a quantum internet are reduced to the levels that are achieved through a fusion splice (<0.08 dB) (this is the widely used process of fusing two fibres together using an electric arc and provides for the lowest loss and least reflectance, as well as providing the strongest and most reliable joint connection between two fibres). Note that splice loss specifications are intended to ensure that the overall link loss is within budget. While system performance is dependent on overall link loss, improved knowledge of an individual component’s overall loss value with all its own intrinsic loss mechanisms can be seen as an important tool for network designers and engineers.

Precision insertion loss measurements are a key parameter that is needed to support manufacturers of high-grade quantum interconnects as part of the traceable quality control process and the successful deployment of these emerging networks.

NPL has existing classical systems that characterize fibre optics and are used for optical communications research. These systems can be modified and applied to quantum-grade or high quality, ultra-low loss optical links and patchcords. These systems can characterize established parameters such as spectral attenuation, insertion loss, return loss, mode field diameter, effective area and numerical aperture. Characterization of these parameters will be vital to provide traceable specifications for any commercial company supplying these high quality and novel fibre types. These would encompass deployment of bend insensitive fibre (G657.A1) Hollow Core Fibre (HCF), Photonic Crystal Fibre (PCF) and few-mode fibre.

Some companies such as Senko Advanced Components (<https://www.senko.com/>), are already producing quantum grade patchcords in FC/UPC, LC, SC, E2000, SN<sup>®</sup> and CS<sup>®</sup> series. These incorporate a commercially available G657.A1 Bend Insensitive fibre with precision made connectors that have been subject to stringent quality controls to qualify as Qu grade (See Appendix 1). It is pertinent to now provide test platforms for key parameters that are capable of low uncertainties commensurate with their quantum level functionality. High end 'classical' systems such as those established at NPL for fibre metrology can play a significant role in characterising specifications required for industry.

In this report we demonstrate the use of our classical systems to characterise these quantum grade patchcords for use in quantum systems. The measurements we are focussing on are insertion loss and MFD. As stated, the prevention and knowledge of the insertion loss of a quantum link is imperative for preventing decoherence and providing stable quantum networks. The MFD of a quantum patchcord can be used to demonstrate the build quality of the patchcord and investigate, how the fibre within the patchcord is affected by the zirconia ferrule in which it is held. As any compression or axial misalignment will lead to losses and decoherence.

The patchcord types we have measured are the E-2000<sup>®</sup> fibre connector and the Senko QuPC connector.

The E-2000<sup>®</sup> fibre connector Figure 1, originally made by Diamond SA, is claimed to demonstrate a repeatable attenuation at the 0.1db level. This is partially due to the use of ceramic ferrules with titanium inserts which use an active crimping alignment process during manufacture. This active process accurately centres the fibre core on the axis of the ferrule thus ensuring insertion loss is minimized.



Figure 1: E-2000® quantum grade APC style connector

The Senko QuPC [3] connector has been designed to emulate the specification for a fusion splice i.e., an insertion loss of less than 0.1 dB and an optical return loss less than 60 dB. This was achieved by improving manufacturing tolerances of the ferrule hole and controlling the apex of fibre curvature during polishing to coincide with the fibre axis while ensuring that fibre undercut, or protrusion is managed.

The pressing need for better standards for quantum grade optical interconnects was demonstrated by the quotation from the cross-standards (ITU, IEC, IEEE, ETSI, BSI) development forum outputs reported in March 2022 that, 'In the short term the most useful standards would be standards for low loss optical interconnect to better allow delicate quantum states, qubits, in the form of single or entangled photons, to be conveyed over longer distances with a lower chance of decoherence and disruption'.

As metrology needs for the Quantum Internet [4] are better understood, the construction of commercially relevant quantum traceable standards become essential. This includes the production of bespoke artefacts to calibrate reference Optical Time Domain Reflectors (OTDR's), Optical Frequency domain Reflectometers (OFDR) and Optical Continuous Wave Reflectometer (OCWR's). However, to achieve the dynamic ranges required ( $>>65\text{dB}$ ), investment in state-of-the-art instrumentation and new methodologies is required to achieve meaningful uncertainties.

We believe that the work in this report is the beginning of creating useful technical standards for both commercial and research purposes.

## 2 Work package overview – ‘Metrology needs for quantum communication networks’

The NMS funded project aims to address key impact and measurable benefits:

- Support UK industry to advance the development of secure quantum communications networks (QCN) and technologies.
- The proposed work will help to identify future collaborative opportunities and develop new metrology capabilities in QCN (e.g.: quantum key distribution (QKD)).
- Dissemination these findings to benefit the wider quantum technologies (QT) community.

Project summary:

The major challenges in the development and deployment of a national secure quantum communications network include the development and deployment of a national secure quantum communications network to include the development, testing and certification infrastructure for QKD devices, novel quantum technologies, and systems. It is essential that NPL is aware of the key design and metrology challenges at an early stage and lead activities by forming strategic partnerships to facilitate deployment of these networks. This project will support these requirements by delivering the 3 milestones below on extending a capability, characterising components as well as dissemination. We will extend the wavelength range of the Variable Launch System (VLS), built during year 3 of this project, to 1310 or 1550 nm to characterise quantum-grade components at wavelength ranges that many photonic based quantum and future comms applications are being designed for. The VLS is capable of characterising both novel optical links designed for quantum networks and also the connectors which are expected to be significant bottlenecks in the wide deployment of quantum networks due their inherent cumulative high losses in legacy communication systems. The project will enable the development of state-of-the-art quantum-grade components in collaboration with our external partner as a leading manufacturer of photonics components for quantum applications.

Milestones:

Year 4:

- Milestone 4 (**Capability**) – Extend wavelength range of the Variable Launch System for characterising coupling efficiency, insertion loss and attenuation to 1310 or 1550 nm. These wavelength ranges are frequently used in future comms and quantum communication applications. (December 2023)
- Milestone 5 (**R&D**) – Test novel quantum grade optical links and connectors from external partner, Senko Advanced Components, at 1310 or 1550 nm. (March 2024)
- Milestone 6 (**Collaboration**) – Measurements to develop classical fibre measurements on the NPL fibre link to the UK quantum network (UKQN). This will allow the QT&E Obj 1 – Capability project to work collaboratively with this project to discover correlations between classical measurements and

exploratory quantum measurements to develop measurement protocols/standards for quantum networks. (Sept 2024)

- Milestone 7 (**Dissemination**) – Publish the methodologies and results in an NPL report. (March 2024)

### 3 Insertion loss measurements on QU grade patchcords

#### 3.1 Commercial criteria

The received commercial quantum grade patchcords from Senko UK incorporated FC/UPC (ultra-polished connector) connectors and were supplied in various lengths. A typical specification sheet supplied with these patchcords is shown in Appendix A. The insertion loss (IL) specification limit of <0.08 dB is listed, this is the expected level of performance commensurate with the worst-case losses associated with a fusion splice (IEC standard reference).

#### 3.2 System build

The methodology of the IL measurements follows current IEC Standards. The relevant standards showed two possible methods that satisfied industry and NPL in its role in carrying out reference measurements. The standard appropriate for industry concerning the measurement of IL is IEC 61300-3-34:2009, whose scope states... 'the procedure required to measure the statistical distribution and mean attenuation for random mated optical connectors'. For obvious reasons, this standard is ideal for batch quality testing of multiple manufactured components. However, for the purposes of reference measurements on a few supplied patchcords such as those described in this report it was felt that the standard IEC 61300-3-4:2013 was more appropriate, whose scope states, 'This part of 61300 describes the various methods available to measure the attenuation of optical components'. In particular, the method chosen was the 'Insertion method (C3) with additional test patchcord'. The schematic below is taken from the standard:

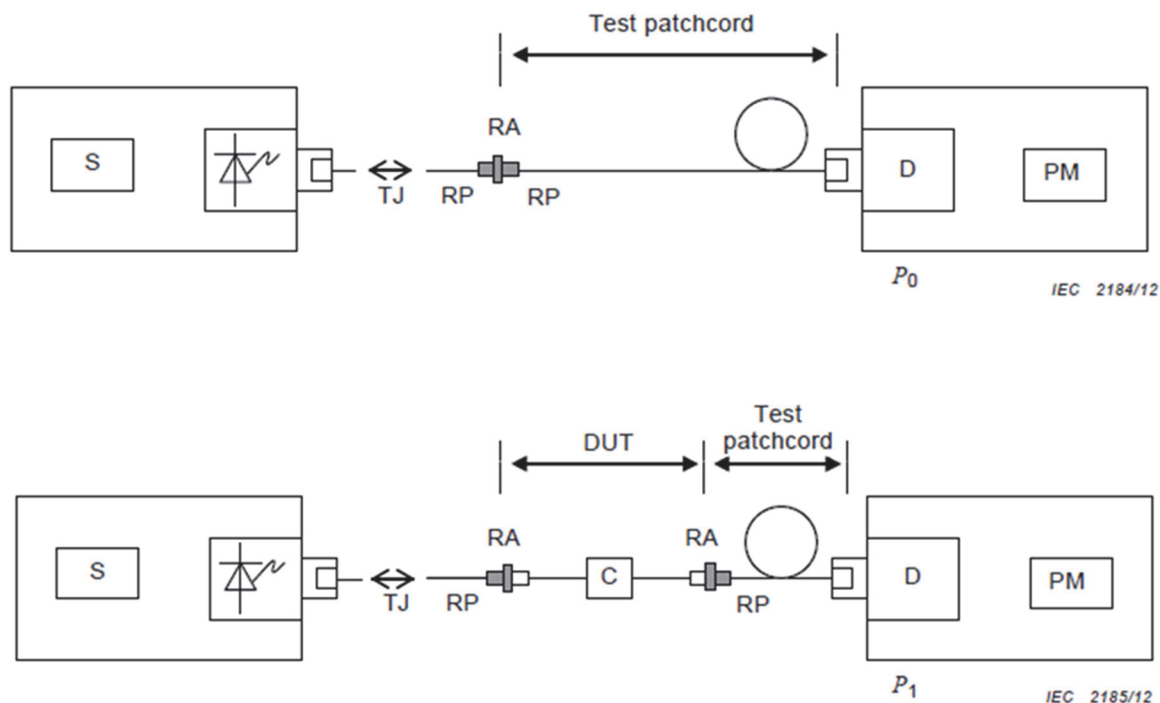


Figure 2: Insertion method (C3) schematic with additional test patchcord



The NPL system follows the above methodology with a few refinements.

The source light goes through an optical attenuator to allow the operator to modify the power of the input.

To check source stability through the measurement stability 10 % of the source is inputted directly to a calibrated power meter, which takes data throughout the measurement.

Finally, instead of using a power meter to detect the power output the NPL apparatus uses a detection system make up of a calibrated transfer standard (Ge69 detector attached to an integrating sphere), a preamplifier and a voltmeter. This optical detection system is the reference system for calibrating power meters so it is higher up the traceability chain to allow for lower uncertainties in the results.

A schematic of the system is shown in Figure 3.

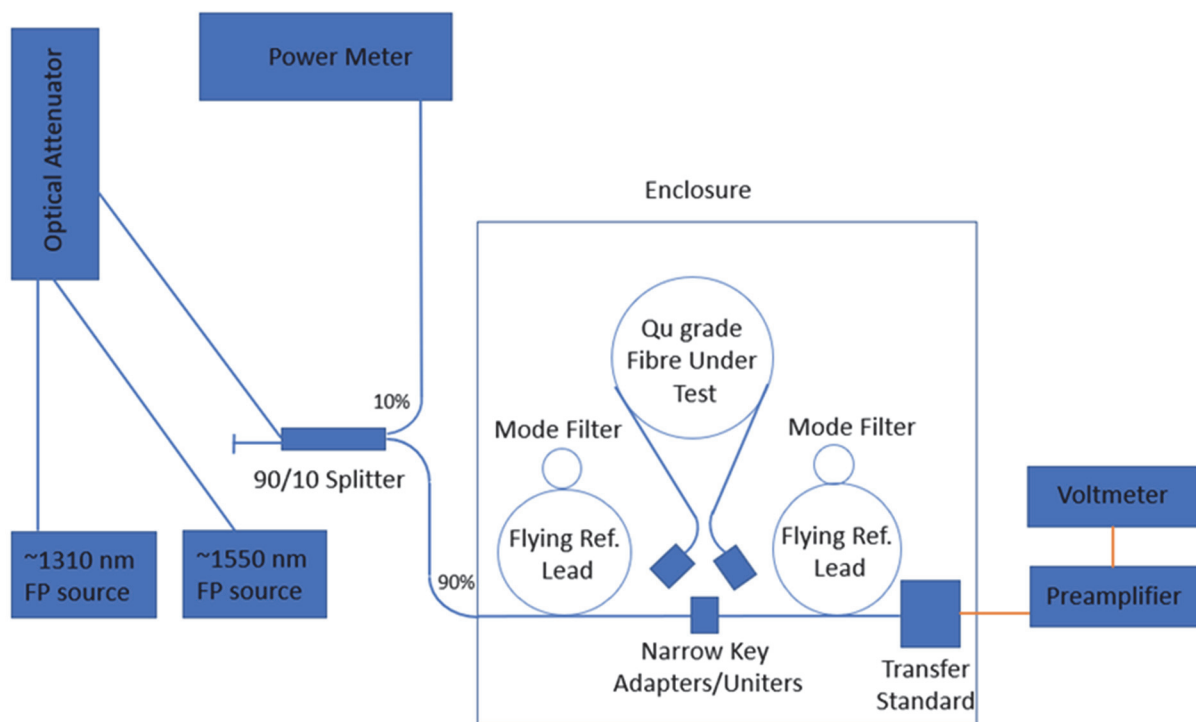


Figure 3 Schematic of NPL Precision Insertion Loss System

The system configuration is as follows:

Thorlabs FP butterfly mounted sources at ~1310 nm (FPL1053S) and ~ 1550 nm (FPL1009S) – mounted in controller model no. CLD 1015

A Viavi optical attenuator (Model No. MAP-220C-A)

Keithley Voltmeter (Model No. 2000)

Transfer standard comprising of a germanium photodetector mounted in an integrating sphere (Model No. JS4)

Vinculum preamplifier (Model No. SP043)

HP fibre optic power meter mainframe with power sensor (Model No.81532A)

PC operating Win10 with LabVIEW software

As part of the measurement methodology significant attention was paid to cleanliness of the fibre patchcord endfaces. Subsequent cleaning and inspection practices and processes were adopted as part of the measurement regime. Fibre optic connectors are susceptible to damage or contamination that is not immediately obvious to the naked eye (See Figure 4). Bad measurements can be made without the user even being aware of a connector problem. An awareness of potential problems, along with good cleaning practices, can ensure that optimum connector performance is maintained.

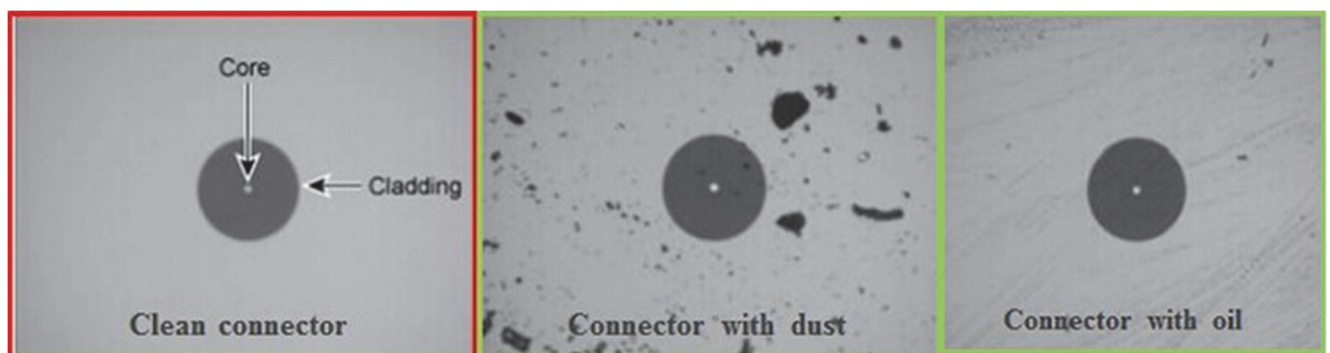


Figure 4: Examples of different types of contamination on connectors.

### 3.3 Software and testing

Software for the measurement of insertion loss using the above system was written in LabVIEW. The software completely controls the measurement, once the user has entered the settings the software collects, processes and saves the data.

There are two types of measurement available within the program, an insertion loss measurement and a measurement of insertion loss across a range of powers.

To make an insertion loss measurement, the software will take voltage readings from the digital voltmeter in the following configurations: without the fibre under test (FUT), with the FUT, with the FUT with ends swapped and without the FUT. The voltage readings are taken a given number of times for repeatability. Once the measurement is complete the voltage readings are converted to power readings in dB and then used to calculate the insertion loss of the fibre as per the standard. This can be repeated as many times as the user wants and then the results averaged to create the insertion loss result.

To take the linearity measurement, the software finds the insertion loss of the fibre at different power levels. For this the measurement happens in four stages, in the first the power through the reference fibre is measured over the given power range, then the power through the FUT is measured over the same range this happens again but with fibre ends swapped around and finally another reference measurement is taken.

This can be repeated as many times as the user wants and the insertion loss results at each power are averaged together for the results.

The instruments in the system are connected via GPIB leads and controlled in LabVIEW using the visa read/write functions. The program is arranged in four modules: main, acquisition, processing and file saving. The main module controls the user interface where the settings are inputted, and the measurement is started. The acquisition module controls the measurement, connects to the instruments, zeros meter sets attenuation and takes data and manages the repeats and number of measurements runs. The data is analysed and processed to insertion loss results in the processing module. The file saving module saves the data to two excel files, a raw data file and results file.

The software has been tested throughout its development to ensure the measurement process is correct and the formulas within the program are correct. The calculations have been verified using the raw data from measurements and inputting them to an excel spreadsheet to perform the same operations.

The following process is followed to calculate insertion loss from the measured voltages.

- First the dark reading is taken from the light to give the voltage reading.
- Where repeat measurements have been taken an average of these repeats is taken.
- This is converted to a power reading in dB using the calibrated electrical responsivity of the germanium detector taking into account the gain setting of the preamplifier.

$$Power\ dB = 10 \times \log \left( \frac{\left( \frac{Voltage \times 10^{gain}}{Responsivity \times 10^{gain-3}} \right)}{1000} \right)$$

- The insertion loss is calculated from the dB powers.

$$Insertion\ Loss = 10 \times \log \left( \frac{Power_{FUT}}{Power_{ref}} \right)$$

### 3.4 Measurements

Following test runs to ensure the operability of the sources, attenuator and detection aspects of the system, more specific tests were carried out to establish system stability, repeatability, and reproducibility of the system as well as to determine the various uncertainty contributions.

In addition, a methodology was adopted that included thorough inspection of the fibre connector endfaces at various stages of the measurement process. Inspection was carried out using a Viavi FV Benchtop Microscope. Cleaning and handling of the connectors was carried out using equipment and techniques developed over many years of experience.

- a) System repeatability – to compare the IL values of a number of simultaneous measurements. Repeatabilities were carried out with the fibres connected as per the reference channel setup only (i.e.: with only the flying leads from the source and the detector and no fibre under test). For each measurement, the connection was separated and re-connected to evaluate the system stability including the repeat activation/setting of the optical attenuator.
- b) System reproducibility – to compare the same IL measurement and setup using different operators on different days.
- c) Uniter contribution – to determine the uncertainty contribution associated with the random selection of high-end uniters/adapters. The uniters chosen were rated as high precision with a narrow keyway.



Figure 5 - FC/PC to FC/PC or FC/APC to FC/APC Single L-Bracket Mating Sleeve, Narrow Precision Key (2.0 mm)

- d) Insertion Loss of FC/UPC Senko 5 m and 10 m Qu grade patchcord – to measure the IL of Qu grade patchcords. The patchcords are measured bi-directionally so that the link is reversed to fully characterise the link with this system.
- e) Insertion Loss of E2000 Senko 5 m Qu grade patchcord – to measure the IL of a Qu grade patchcord. The patchcord is measured bi-directionally so that the link is reversed to fully characterise the link with this system.
- f) Linearity – to investigate the IL values across a range of power levels. To see whether the performance of the Qu grade patchcord is affected, particularly at lower power levels as this is more relevant to the functional performance to do with the transmission of entangled photons. More relevant would be to compare the linearity values obtained with this ‘classical’ system and those from a system incorporating single photon avalanche detectors (SPAD) and spontaneous parametric down-conversion (SPDC) sources. This is highly desirable as it allows the possibility to produce a complete view of linearity performance of a Qu grade link from ‘classical’ to quantum levels.

### 3.5 Results

Two FC/UPC Senko Qu grade patchcords, 5 m length - NPL ID: 4 (SN: M-22020563-21210) and 10 m length - NPL ID: 6 (SN: M-22020563-21206) were measured at the wavelengths 1310 and 1550 nm at a power of – 10 dBm by three operators. The results are shown below:

**Table 1. ID 4 at 1310 nm**

End A Insertion Loss dB	End B Insertion Loss dB	Average Insertion Loss dB	Uncertainty %
0.017	0.023	0.020	0.55
0.017	0.008	0.013	0.45
0.027	0.028	0.028	0.42

**Table 2. ID 6 at 1310 nm**

End A Insertion Loss dB	End B Insertion Loss dB	Average Insertion Loss dB	Uncertainty %
0.031	0.034	0.033	0.39
0.024	0.021	0.023	0.41
0.032	0.025	0.029	0.43

**Table 3. ID 4 at 1550 nm**

End A Insertion Loss dB	End B Insertion Loss dB	Average Insertion Loss dB	Uncertainty %
0.056	0.035	0.045	0.83
0.025	0.025	0.025	0.65
0.058	0.014	0.036	1.37

**Table 4. ID 6 at 1550 nm**

End A Insertion Loss dB	End B Insertion Loss dB	Average Insertion Loss dB	Uncertainty %
0.019	0.027	0.023	0.73
0.019	0.016	0.018	0.66
0.014	0.030	0.022	0.77

Two E2000 Senko 8 m Qu grade patchcords, (SN: 35020002 and NPL ID: 7) and (SN: 35020001 and NPL ID: 8) was measured at the wavelengths 1310 and 1550 nm by three operators. The results are shown below.

**Table 5. ID 7 at 1310 nm**

End A Insertion Loss dB	End B Insertion Loss dB	Average Insertion Loss dB	Uncertainty %
0.221	0.158	0.190	1.68
0.276	0.142	0.209	3.41
0.247	0.146	0.197	2.62

**Table 6. ID 8 at 1310 nm**

End A Insertion Loss dB	End B Insertion Loss dB	Average Insertion Loss dB	Uncertainty %
0.044	0.075	0.060	0.90
0.024	0.065	0.045	1.16
0.017	0.068	0.043	1.40

**Table 7. ID 7 at 1550 nm**

End A Insertion Loss dB	End B Insertion Loss dB	Average Insertion Loss dB	Uncertainty %
0.186	0.119	0.152	1.85
0.202	0.096	0.149	2.81
0.165	0.096	0.131	1.94

**Table 8. ID 8 at 1550 nm**

End A Insertion Loss dB	End B Insertion Loss dB	Average Insertion Loss dB	Uncertainty %
0.037	0.068	0.052	1.04
0.037	0.060	0.049	0.90
0.026	0.063	0.045	1.16

### 3.6 Treatment of uncertainties

To create the uncertainty budget for this measurement we developed from the established budget used in the UKAS accredited power meter calibration service which uses the same germanium detector/integrating sphere set up.

We tailored this to the measurement by removing part specific to that measurement and adding factors based on repeatability and reproducibility.

An example budget based on an insertion loss measurement, with 5 repeats, at 1310 nm is at one patch cord is as follows:

**Table 9. Uncertainty budget for measurements**

Source	Type	Value %	Distribution	Divisor	Ci	U <sub>i</sub>	V <sub>eff</sub>
FUT repeatability	A	0.062	normal	1	1	0.062	4
Ref repeatability	A	0.056	normal	1	1	0.056	9
Detector Calibration	B	0.490	normal	2.09	1	0.234	30
Voltmeter	B	0.020	normal	2	1	0.010	Inf
Op Amp calibration	B	0.020	normal	2	1	0.010	Inf
Source wavelength	B	0.050	rectangular	1.732	0.3	0.009	Inf
Temperature effects	B	0.010	rectangular	1.732	2	0.012	Inf
Humidity effects	B	0.010	rectangular	1.732	20	0.115	Inf
Polarisation effects	B	0.000	rectangular	1.732	1	0.000	Inf
<b>Combined Uncertainty %</b>						<b>0.28</b>	<b>54</b>
<b>Expanded Uncertainty % (k=2.05)</b>						<b>0.57</b>	<b>54</b>

The uncertainty budget combining the uncertainties of a measurement of both ends of a patch cord is as follows:

**Table 10. Combined uncertainties of the measurements**

Source	Type	Value %	Distribution	Divisor	Ci	U <sub>i</sub>	V <sub>eff</sub>
End A Uncertainty	B	0.275	Normal	1	0.5	0.138	54
End B Uncertainty	B	0.271	Normal	1	0.5	0.136	53
Difference between Ends	B	0.259	Rectangular	1.732	1	0.149	Inf
<b>Combined Uncertainty %</b>						<b>0.24</b>	<b>273</b>
<b>Expanded Uncertainty % (k=2.01)</b>						<b>0.49</b>	<b>273</b>

The uncertainty sources are explained as follows:

#### FUT/Ref Repeatability

This is the repeatability of the power measurements of the system with and without the fibre under test respectively is taken to be the standard error of the mean of the calibration results.

#### Detector Calibration

This is the contribution arising from the uncertainty in the calibration of the transfer standards at NPL.



#### Voltmeter

This is the contribution from the voltmeter reading. This is calibrated with an uncertainty of 0.02%.

#### Op Amp calibration

The current generated by the germanium and JS detectors is converted to a voltage and amplified. The gain of the op-amp that performs this task is calibrated with an uncertainty of 0.02%.

#### Source wavelength

This is the contribution arising from the uncertainty in the source wavelength that is used for the calibration and the spectral sensitivity of the detector to a wavelength region.

#### Temperature/Humidity of transfer standards

The temperature and humidity sensitivity of the detector used.

#### Polarisation effect

Integrating sphere-based detectors are generally considered to be intrinsically polarisation insensitive.

The largest contribution to the uncertainty of a measurement comes from the variation of the measured values and the variation between each end of the fibre. This makes sense as the source is stable, and you won't expect the insertion loss of fibre to change as you turn it round.

Any large variation in these can be assumed to come from disruption of the experimental set up for example dirt getting into the system. However, some variation is expected due to the variables of how a patchcord is connected, tension angle etc, which can affect the signal on input and output.

Understanding this, the measurement process included the operator disconnecting and reconnecting the end of the fibre under test to ensure a repeatable connection and insertion loss profile. Further to this the process of using multiple users allowed for the demonstration of how a different operator may use a patchcord and how that can affect the results.

### 3.7 Linearity

In addition to the insertion loss measurements carried out at – 10 dBm on the commercial Qu grade patchcords, work was carried out to assess the linearity of the system and to develop the capability to characterise how the insertion loss of a patch cord changes as the input power decreases. This will provide a further advantage in characterising performance as source signals are varied and can be combined with quantum level loss measurements to provide a complete range of linearity values from classical to quantum levels.

This measurement used the linearity part of the program written for the insertion loss measurement. To ensure the input power was linear a calibrated germanium detector (Ge69) was used to measure the power output of the system, this detect was cooled to -20 °C as is known to be linear from 10 dBm to -90 dBm.

The graph below shows the variation in insertion loss over a power range of -10 dBm to -90 dBm at a wavelength of 1310 nm for a 10 m QuPc Senko patch cord ID6.

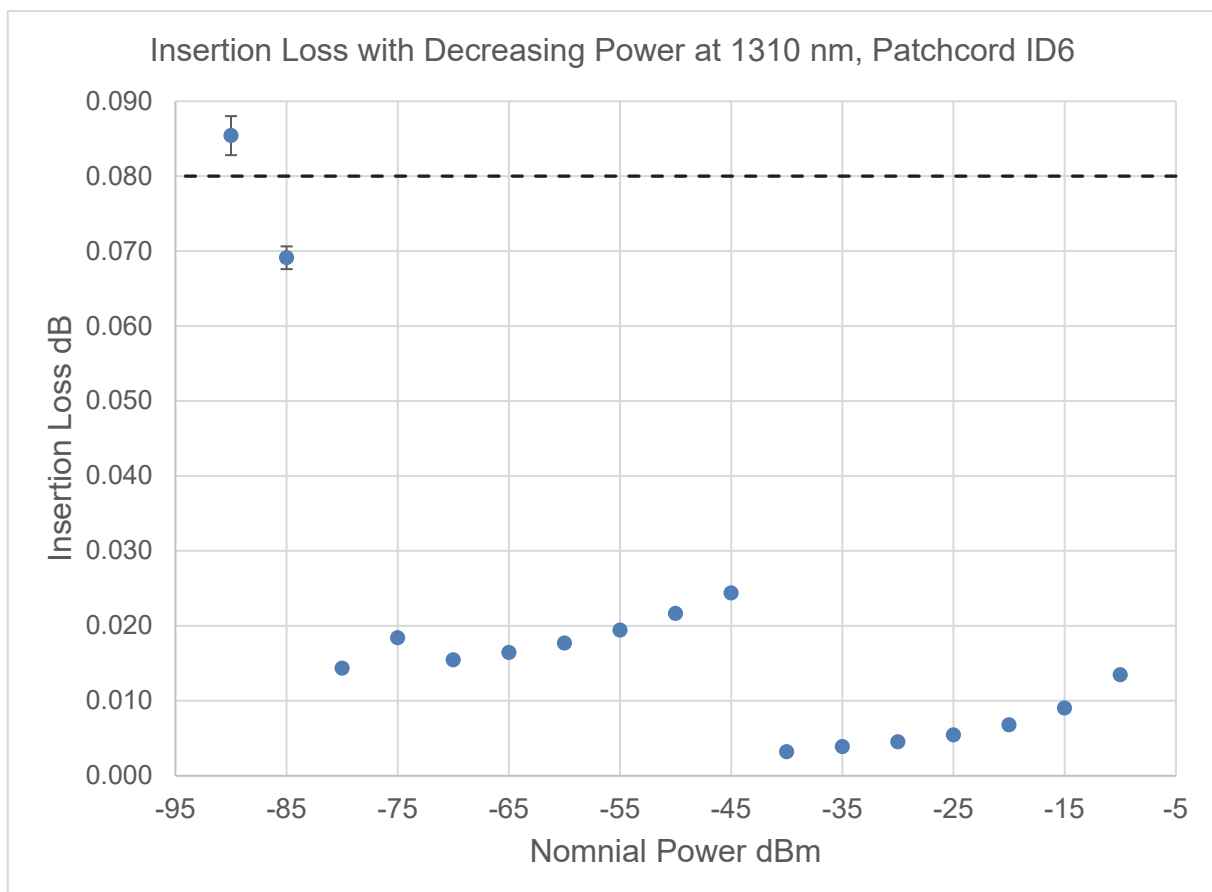


Figure 6 Graph showing variation in insertion loss over power range of -10 dBm to -90 dBm.

The graph shows that the insertion loss of the patchcord remains within the manufacturers specification up to the noise floor of the measurement system at -90 dBm.

Looking at the graph we see an increase in insertion loss at the -45 dBm point, this can be attributed to the measurement procedure where an extra fixed attenuator is

used so that the lower attenuation ranges can be achieved. At the lowest powers of -85 dBm and -90 dBm there is a further increase with the -90 dBm being outside the manufacturer's specification. This is because these measurements are taken in the noise floor of the detection system making the insertion loss harder to measure and increasing the variance of the data.

### 3.8 Summary

For the FC/UPC Senko 5 m (NPL ID: 4) and 10 m (NPL ID: 6) Qu grade patchcords, the results showed good agreement with the commercial specification. The NPL IL average values are shown compared to the commercial specification for these fibres:

**Table 11. Results at ~1310 nm**

NPL ID:	Senko mean IL values (dB)	NPL mean IL values (dB)	IL Difference (dB)	IL Difference (%)
4	0.025	0.0203	0.0047	0.11
6	0.035	0.0283	0.0067	0.15

**Table 12. Results at ~1550 nm**

NPL ID:	Senko mean IL values (dB)	NPL mean IL values (dB)	IL Difference (dB)	IL Difference (%)
4	0.045	0.0353	0.0097	0.22
6	0.015	0.0210	0.0060	0.14

For the E2000 Senko 8 m ((NPL ID: 7) SN: 35020002) and (NPL ID: 8) SN:35020001 Qu grade patchcords, the NPL ID: 8 results showed reasonable agreement with the commercial specification. The results for NPL ID: 7 were significantly different. The NPL IL average values are shown compared to the commercial specification for these fibres:

**Table 13. Results at ~1310 nm:**

NPL ID:	Senko mean IL values (dB)	NPL mean IL values (dB)	IL Difference (dB)	IL Difference (%)
7	0.040	0.1987	0.1587	3.72
8	0.090	0.0490	0.041	0.95

**Table 14. Results at ~1550 nm:**

NPL ID:	Senko mean IL values (dB)	NPL mean IL values (dB)	IL Difference (dB)	IL Difference (%)
7	0.035	0.1440	0.109	2.54
8	0.085	0.0480	0.037	0.86

For the FC/UPC patchcords, the results show very good consistency and agreement with commercial specifications. However, this is not the case for both the E2000 patchcords where one exhibits significantly higher IL values and associated uncertainties. In particular, for NPL ID: 7, the NPL values for the E2000 patchcord clearly fall outside the notional specification of 0.08 dB. Control measurements were carried out using replacement, new Diamond E2000 adapters which were consistent

with the above values. This showed that the adapters used during the measurements were not of poor quality or faulty. However, for NPL ID: 8 the values are much more in-line with expected IL values.

In conclusion, the variation between NPL ID: 7 and NPL ID: 8 is significant as it suggests that there is inconsistency in the build quality or possibly, the commercial measurements for the E2000 type of patchcords. This difference is relatively large and requires further investigation. Higher insertion losses could be attributed to inferior build quality of the E2000 connectors when compared with the FC/UPC connectors, although clearly, this would require much more comprehensive investigation. The differences between the two ends of NPL ID: 7 is also larger than those of the FC/UPC patchcords and subsequently significantly increases the expanded uncertainties. In conclusion, the adoption of E2000 patchcords within quantum networks needs to be questioned as there is the potential that they could lead to unacceptable system losses. The limited scope of this project prevents major conclusions regarding the E2000 connectors; however, further metrology is needed to determine more fully the causes of this variance.

## **4 Mode field diameter on Qu grade patchcords**

### **4.1 Commercial criteria**

In addition, fibre geometry services have the potential to assess quantum grade connectors and the associated parameters of cladding diameter, non-circularity and core-cladding concentricity of the fibre with respect to the Zirconia ferrule and the mechanical build quality of high-grade connectors.

The transmission of entangled photons over long distances is dependent on the build quality of commercial connectors, this involves a range of considerations if coupling efficiencies are to be maintained. Axial alignment of the fibre with respect to the zirconia ferrule and surrounding manufactured connector housing is one such area of concern as is core cladding concentricity of the fibre. Another area of concern is the compression that the zirconia ferrule imposes on the fibre core and the subsequent effect it may have on MFD, i.e., the guided width of the fundamental mode. Non-circularities of the MFD can be a significant cause of core mismatching between connectorized links which can increase decoherence by affecting the polarisation of the entangled photons. Measurements of MFD using the far-field scanning technique can assess the build performance of commercial connectors therefore providing direct support for industry.

Fibre connectors are designed to produce a reproducible connection between two fibres, by mechanically aligning the cores of the fibres with each another. The standard metric of connector performance is insertion loss, commonly tested against an "ideal" reference connector. Most connectors are made with a precision drilled hole in a cylindrical ferrule. The stripped and cleaned fibre is inserted into the hole in the ferrule which is filled with epoxy.

When the fibre connectors are pushed together, the ferrules are aligned in a sleeve; if the fibre cores lie on their correct respective ferrule axes, aligning the ferrules produces fibre core alignment.

Errors in lateral alignment are produced when the fibre cores are eccentric compared with the ferrule axis. This physical core mismatch in addition to any differences between the intrinsic mode field diameters of connected links form the largest contributions to insertion loss in single-mode connectors. The NPL Far-Field Scanning system used to characterise Mode Field Diameter is a flexible platform that can accommodate these emerging 'Qu' grade links providing low uncertainties and information regarding the mean diameter and non-circularity of the mode field.

Mode Field Diameter (MFD) is a measure of the width of the guided mode in the fibre. Consequently, it depends on the parameters which affect guiding, such as the refractive index difference between the core and cladding, core diameter and wavelength. Typical values are around 10  $\mu\text{m}$ . Mode field diameter is a key parameter because the radial extent of the mode can be used to predict losses at joints and microbends within communication networks. In addition, if its spectral variation is known, it can be used to measure cut off wavelength. Other parameters

which can be predicted using MFD data include waveguide dispersion and refractive index profile. From the far-field scans obtained for the measure of MFD, the effective area of the core can also be obtained. The MFD is a measure of the radial extent of the guided mode in the fibre. The definition of MFD which is used is the Petermann II definition which involves calculating a weighted mean of the angular intensity distribution in the far field. The far field scan technique involves coupling light into a short length of the fibre under measurement and scanning a detector in the far field in a circular arc centred on the fibre end face. The detected intensity with respect to angular position is recorded and this data is used to calculate the MFD. Measurements are possible from 1250 to 1625 nm, however results at 1310 nm and 1550 nm are usually quoted.

## 4.2 Far-field system overview

The most straight forward method of measuring MFD is to measure  $P(\theta)$  in the far-field by scanning a detector around an arc centred on the end of the fibre under measurement and compute the MFD according to Equation 1. The far field scan technique is the preferred method for the measurement of circularly symmetric fibres and is the techniques used at NPL to measure MFD for customers [5]. A schematic diagram of such a setup is shown below.

Eq. 1

$$2 w_{ff} = \left( \frac{\lambda}{\pi} \right) \cdot \left[ 2 \frac{\int_0^{\theta_{max}} P(\theta) \sin \theta \cos \theta d\theta}{\int_0^{\theta_{max}} P(\theta) \sin^3 \theta \cos \theta d\theta} \right]^{\frac{1}{2}}$$

Equation 1 shows the Petermann II definition. What is required is a definition which makes no assumptions about the field distribution, which can be used to predict the loss mechanisms mentioned above and which is applicable to various measurement techniques without the need for complicated transforms. The Petermann II definition which has been adopted by specification standards bodies satisfies these requirements. Intercomparisons of MFD measurements have shown that this definition of MFD gives a good agreement of measured MFD values when used to evaluate MFD from data obtained from different measurement techniques.

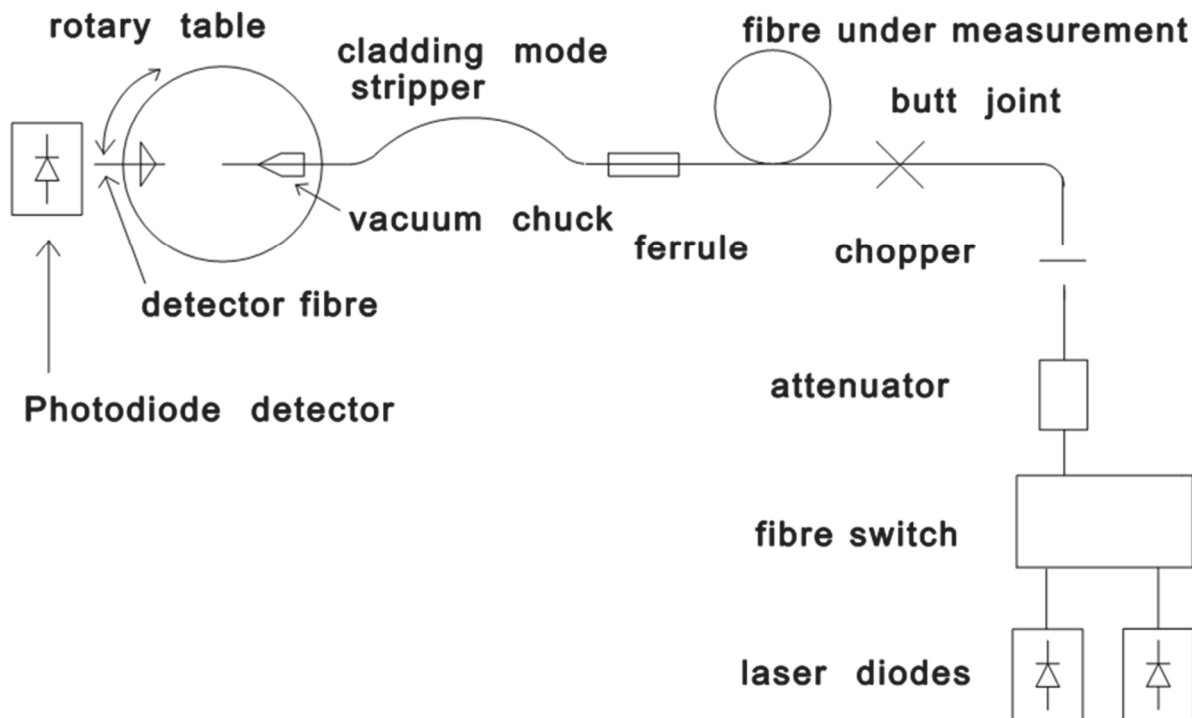


Figure 7 - Schematic of the far-field system to measure MFD at NPL



The sources are usually laser diodes to provide enough signal in the far-field especially at high angles. Measurements are usually made around 1310 nm and 1550 nm. The output of the fibre pigtailed lasers is coupled into a few metres of the fibre under measurement. A single turn of the fibre around a ~ 25 mm diameter rod placed after the splice is used to remove any high order modes and a cladding mode stripper is used immediately before the end of the fibre. The detector is mounted on a rotation stage and scanned round an appropriate angle, in small angular steps, measuring the power,  $P(\Theta)$ . To ensure that the detector is in the far-field the separation between fibre and detector need only be greater than 1 mm, however, to ensure good angular resolution the detector is often a few centimetres from the fibre. The size of the detector is another factor which determines the angular resolution, the fibre pigtail of a photodiode can provide a small area detector allowing the fibre-detector distance to be reduced without loss of angular resolution. The criterion for fibre-detector separation is that it should be greater than 10 mm and greater than  $\sim 125b$ . Here,  $b$  is the diameter of the active area of the detector and  $\lambda$  is the wavelength.

A typical scan produced by a far field system built at NPL on a G.652.D type fibre is shown below. The intensity is shown on the vertical axis in dB with angular position in degrees on the horizontal axis.

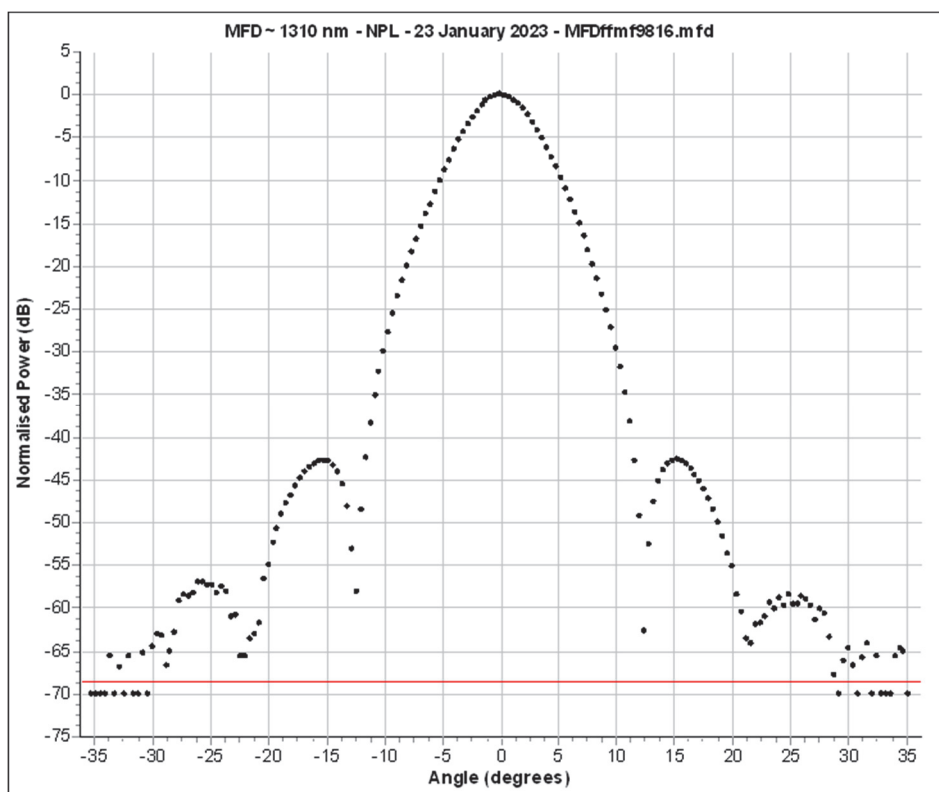


Figure 8: Typical MFD measurement showing the far-field scan at ~1310 nm

For this step-index fibre whose MFD is approximately  $9 \mu\text{m}$ , the side lobes at approximately  $\pm 13^\circ$  are zero crossings of the electric field; that the intensity at those zero crossings does not go approximately below  $-65 \text{ dB}$  is a measure of the scattered light in the system. For the NPL system, measurements are possible from 1250 to 1625 nm, however, results at 1310 nm and 1550 nm are usually quoted. The

far field scan system constructed at NPL can measure MFDs in the range 3.5 - 13  $\mu\text{m}$ . The best uncertainty which can be achieved by the system is  $\pm 0.6\%$ . The mode field diameter non-circularity (defined as the difference between the largest and smallest MFD divided by the mean MFD expressed as a percentage) is also measured with a best measurement uncertainty of 0.1%.

### 4.3 Modifications

The system at NPL was designed to measure bare samples of single-mode fibre to a best measurement capability of  $\pm 0.06 \mu\text{m}$  at c. 1310 nm and c. 1550 nm and is readily available as a measurement service for classical long-haul fibres.

Modifications were made to the system to accommodate a high quality, commercial connector used for quantum applications.

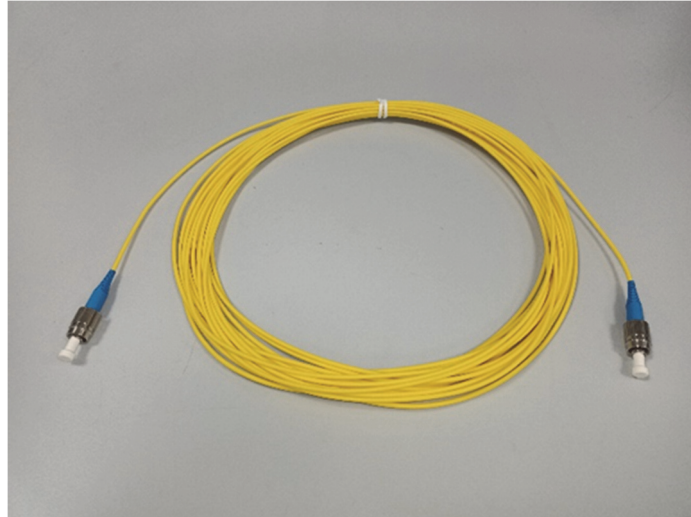


Figure 9 - Commercial Qu grade FC/UPC patchcord (10 m)

The patchcord supplied was a FC/UPC (Flat connector/Ultra polished connector) Senko 10 m Qu grade patchcord, NPL ID: 5 (SN: M22020563-21207). The actual fibre type used within the patchcord build was a commercially available G.657.A1 Bend Insensitive fibre.

A suitable adapter was designed and developed to securely hold the precision connector end of the 10 m patchcord, without compressing the fibre which could affect the mode field measurement. In addition, the connector needed to be rotated to allow the assessment of the non-circularity of the MFD, crucial, if important assessments of core mismatch are to be made. Once mounted, a process was developed to correctly align with the detector fibre mounted within a frustum cone. A far-field 2D profile was then measured by moving the detector fibre through an angle of around  $\pm 35$  degs to produce an intensity profile that was analysed using the internationally agreed integral to determine the MFD value (Petermann II definition).

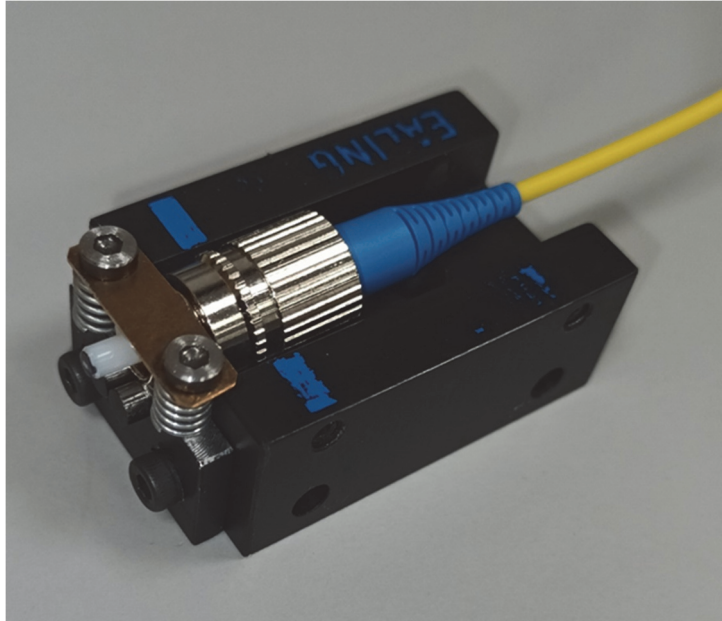


Figure 10 - Qu grade connector mounted in modified adapter.

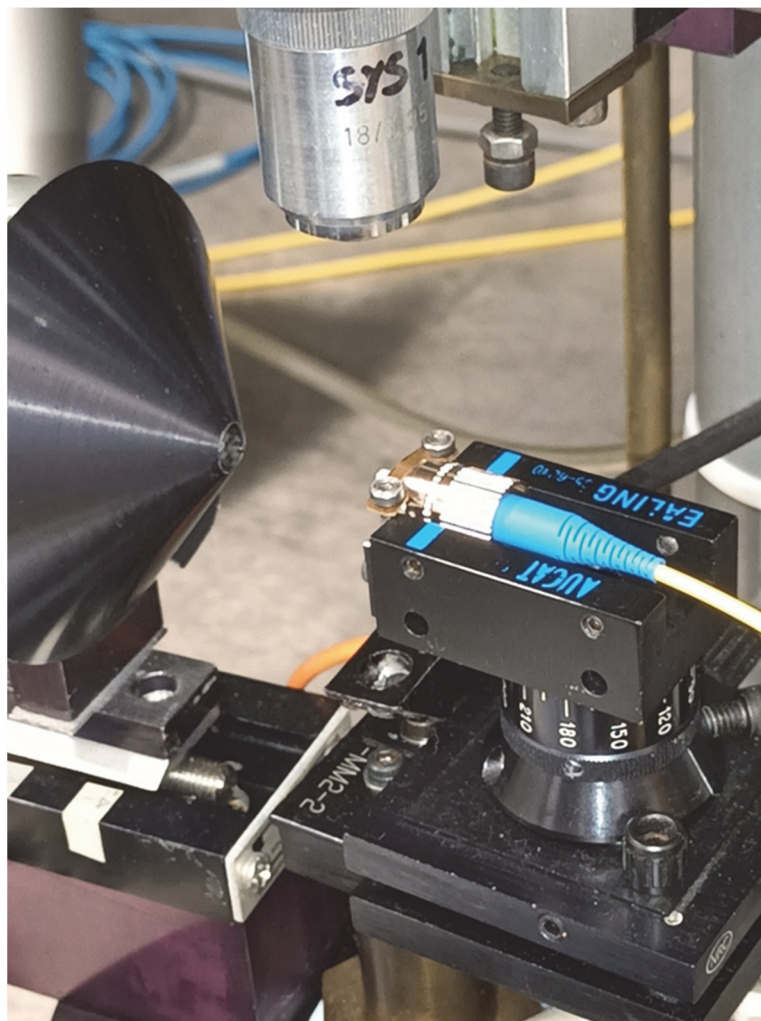


Figure 11 - Qu grade connector mounted in modified adapter on MFD system

#### 4.4 Measurements

Time was spent obtaining the best alignment of the end face of the fibre under test and the detector fibre mounted within the frustum cone to minimise the offset and asymmetry uncertainty contributions. Large values for offset and asymmetry would also lead to incorrect MFD values. This proved difficult as the system is designed to align bare fibres, however, by modifying the alignment process to optimise the signal levels on the systems' Phase Signal Detector (PDS) it was possible to carry out measurements that were comparable to those for bare fibre samples and which compared to the systems ~25 years of historical values.

As well as the issue of alignment, there was concern that the front facet of the zirconia ferrule that surrounds the actual fibre would reflect light back into the detector fibre and result in a reduced signal to noise ratio (SNR) effectively curtailing the systems' dynamic range. Initially, a pinhole was mounted in front of the ferrule, but this proved cumbersome and effectively vignetted the Numerical Aperture (NA) of the fibre output. Following this, an indelible ink pen was used to carefully apply a mask around the fibre. Subsequent measurements found that the use of an 'anti-reflection' coating exhibited no noticeable difference to the far-field intensity plot. This may well be because the ferrule end facet is significantly convex and diverges any light that might otherwise reach the detector fibre.

Measurements were made on the Qu grade patchcord at ~ 1310 nm and ~1550 nm. At both wavelengths five measurements were made on the fibre, rotating it 45° around its axis between each measurement and the scan angle was set at  $\pm 35.2^\circ$  following a convergence check (This is carried out by performing the first scan with a wide angular range, i.e.,  $\pm 44^\circ$ . The current version of the convergence program is used to analyse the way in which MFD converges with scan angle. The scan angle for subsequent scans should be chosen so that it is large enough to give a MFD within 0.003  $\mu\text{m}$  of the wide-angle value). The calculated mode field diameter is the average of these measurements. A cladding mode stripper was employed before the output end of the patchcord. The data was used to calculate the mode field non-circularity. To correct the measured wavelengths to 1310 nm and 1550 nm additional measurements were carried out. The rate of change of MFD with wavelength should be known to correct the MFD to the appropriate wavelength. In most circumstances it is sufficient to use the rate of change of MFD between 1310 nm and 1550 nm to make any small corrections.

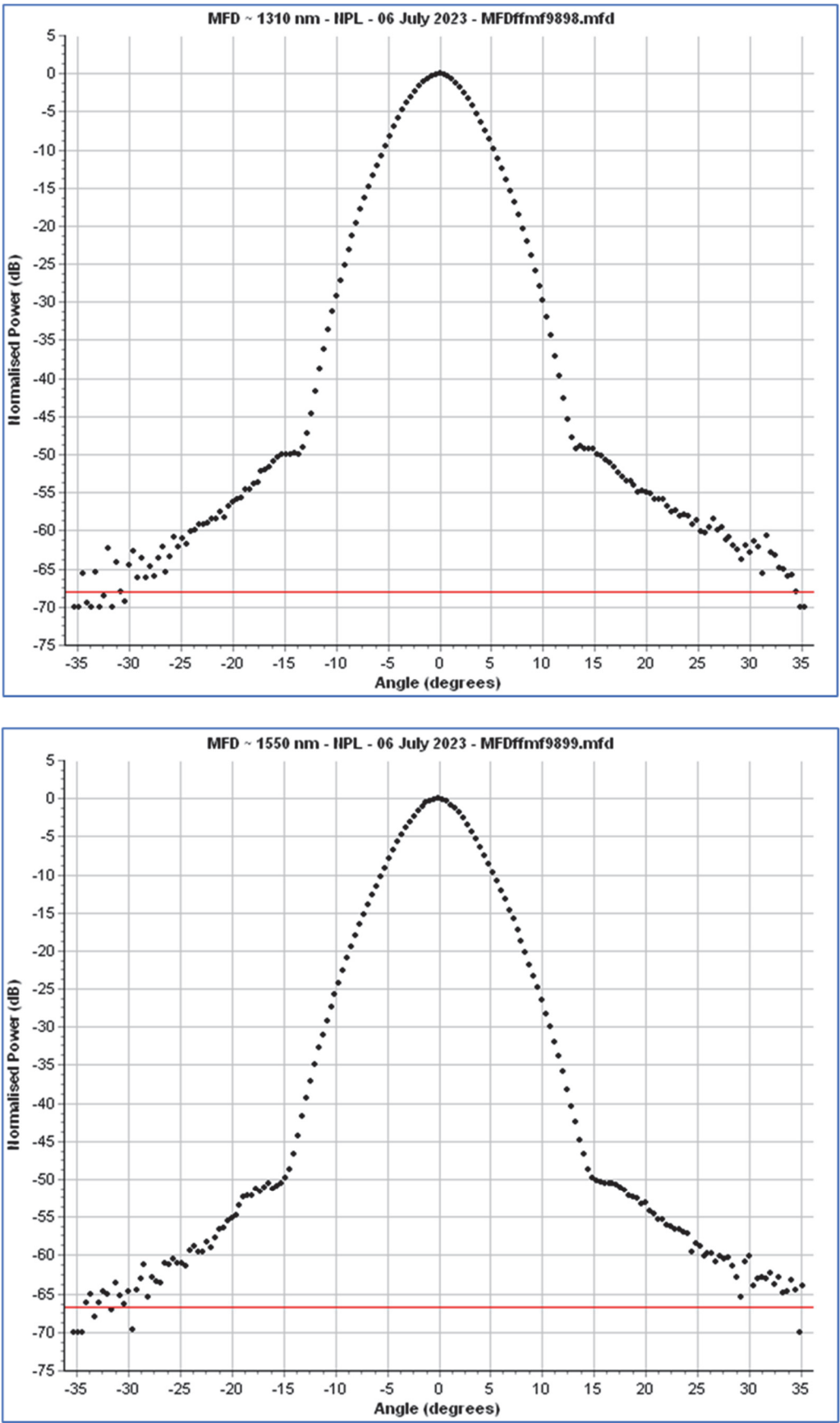
## 4.5 Results

The processed results are shown below. These include the measurements made at specific wavelengths and the values corrected to 1310 nm and 1550 nm.

<b>Matched Clad Bare Fibre MFD Calculation (Version 4.2a)</b>							
<b>Date:</b>	7 July 2023						
<b>LIM S Ref:</b>	N/A		<b>Wavelength 1:</b>	1309.9	nm		
<b>Cert Ref:</b>	N/A		<b>Wavelength 2:</b>	1549.9	nm		
<b>Customer:</b>	SENKO/NPL		<b>Wavelength 3:</b>	1327.7	nm		
<b>Fibre ID:</b>	Senko 10 m		<b>Wavelength 4:</b>	1525.7	nm		
<b>RESULTS</b>	<b>MFD (microns)</b>	<b>+/- (microns)</b>	<b>Non Circ %</b>	<b>+/- %</b>	<b>Non Circ &lt; %</b>		
1310 nm	9.165	0.06	0.14	0.12	0.26		
1550 nm	10.297	0.07					
<b>UNCERTS</b>	<b>MFD / Non Circ</b>	<b>Sn-1</b>	<b>SEM (%)</b>	<b>Stat +Syst</b>	<b>Deg Freedom</b>	<b>k</b>	<b>U95Tot</b>
1309.9	9.1652	0.00369728	0.012756779	0.320254173	100.3117615	1983971519	0.64
1549.9	10.2968	0.01364058	0.04189191	0.322730433	102.7028481	1983495259	0.64
%	0.14	0.06377042	0.031885211	0.056419028	16.10884954	2.119905299	0.12
<b>END A</b>	N/A	<b>Fringes.</b>					
<b>Orientation</b>	<b>MFD@1309.9</b>	<b>A sym m</b>	<b>File (FFMF)</b>	<b>MFD@1549.9</b>	<b>A sym m</b>	<b>File (FFMF)</b>	
0	9.1651	-0.15	9898	10.3062	-0.213	9899	
45	9.1617	-0.205	9900	10.3085	-0.219	9901	
90	9.1681	-0.226	9902	10.3124	-0.133	9903	
135	9.1655	-0.125	9904	10.3096	0.004	9905	
180	9.1646	-0.261	9906	10.301	0.261	9907	
<b>Number</b>	5			5			
<b>Average</b>	9.1650			10.3075			
<b>Sn-1</b>	0.0023			0.0043			
<b>Non-Circ</b>	0.0065			0.0115			
<b>Non-Circ (%)</b>	0.08			0.12			
<b>END B</b>	N/A	<b>Fringes.</b>					
<b>Orientation</b>	<b>MFD@1309.9</b>	<b>A sym m</b>	<b>File (FFMF)</b>	<b>MFD@1549.9</b>	<b>A sym m</b>	<b>File (FFMF)</b>	
0	9.1664	0.244	9916	10.2792	-0.284	9917	
45	9.1738	-0.068	9918	10.3002	-0.03	9926	
90	9.1621	-0.276	9920	10.2769	-0.342	9921	
135	9.1625	-0.285	9922	10.2794	-0.323	9923	
180	9.1621	-0.274	9924	10.2947	-0.022	9925	
<b>Number</b>	5			5			
<b>Average</b>	9.1654			10.2861			
<b>Sn-1</b>	0.0051			0.0107			
<b>Non-Circ</b>	0.0117			0.0234			
<b>Non-Circ (%)</b>	0.13			0.23			
<b>WAVELENGTH DEPENDANCE</b>							
<b>Wavelength</b>	<b>MFD</b>	<b>File (FFMF)</b>	<b>micron/nm</b>				
1309.9							
1327.7			0.0029	Mean of End A and End B			
1525.7							
1549.9			0.0062	Mean of End A and End B			



Figure 11 - Typical scans for ~1310 nm and ~1550 nm



## 4.6 Conclusions

The MFD values were commensurate with values associated with commercial G.657.A1 fibre ( $\sim 9.17\mu\text{m}$  @ 1310 nm and  $\sim 10.30\mu\text{m}$  @ 1550 nm) however, it was noted that the measured values were at the higher end of the commercial specification for this type of fibre and in some cases outside the upper bound.

**Table 15. Examples of commercial specifications**

Commercial Specification	MFD Specification at 1310 nm ( $\mu\text{m}$ )	MFD Specification at 1550 nm ( $\mu\text{m}$ )
1	$8.6 \pm 0.4$	$9.6 \pm 0.5$
2	$9.0 \pm 0.4$	$10.1 \pm 0.5$
3	$8.8 \pm 0.4$	$9.8 \pm 0.5$
4	$8.9 \pm 0.4$	N/A
IEC 60793-2-50:2018	Nominal MFD range 8.6 to 9.2 Tolerance $\pm 0.4$	N/A

It is possible that compression caused by the zirconia ferrule and the curing of the adhesive that secures the fibre has caused the apparent minor increase in MFD. This is complicated by the fact that due to diffraction, small MFD's tend to produce broad far-field patterns and that the angular scan of the measurements did not show any truncation that would mean the signal at higher scan angles would be lost. If the core was effectively constricted, then this would have a slight effect on the densities of the core and cladding resulting in possible changes in refractive index differences. This could explain the measurements that are at the upper end of the tolerance band for this type of fibre. The best solution would be to remove the connectors and re-measure the bare fibre to compare the values to better understand the possible impact of the connector ferrules.

Non-circularities for each end at both wavelengths ranged from 0.08% to 0.12% (End A) and 0.13% to 0.23% (End B). This is not un-typical of commercially available G.652.D which G.657.A1 is largely similar to. However, what was apparent (and not unexpected), was the flattening of the far-field mode field profile from around  $\pm 15^\circ$  to  $\pm 35^\circ$ . MFDs measurements on fibre mounted within a retractable holder for use on commercial MFD instruments also exhibit this flattened profile.

Constriction of the fibre by the surrounding zirconia ferrule has been shown to depress the electric field inversion points on the far-field profile thus affecting the definition of the side-lobes. These correspond to points where the electric field amplitude has changed sign between positive and negative. They are identified by distinct discontinuous nulls in the measured intensity distribution where the field amplitude passes through zero. Depending on the level of random noise in the measured data, it may be possible to identify one, two or three side-lobe nulls to either side of the main peak. The side lobes commonly found in far-field scans are recorded as positive intensity points but correspond to the square of negative amplitude values.

Note that in analysing the far-field data, the absolute values of the measured intensities were used to avoid producing imaginary amplitude values in the noise floor (For the calculation of the effective area from the far-field data, the square root



of the intensities were taken, the side lobes were located manually and the amplitude of the odd numbered lobes inverted). This is important to note as this has the potential to affect the MFD and poses a significant quality risk in the construction of quantum grade connectors.

Careful consideration of fibre/ferrule selection and of the processes of construction (that maintain and control core-cladding/ferrule/connector concentricity) and selection that are needed to avoid any loss of functionality of these links at the quantum level.

#### 4.7 Uncertainty contributions

A summary of the contributions to the measurement uncertainty for matched clad fibres is given in table 16 below.

**Table 16. MFD Uncertainty budget for matched clad fibres**

Symbol	Para. Ref.	Source	Value $\pm$ %	Prob. Dist <sup>n</sup> .	Div.	C <sub>i</sub>	u <sub>i</sub> $\pm$ %	v <sub>i</sub>
$\sigma_{LIN}$	13.1.2	System Linearity	0.32	R	$\sqrt{3}$	1	0.20	$\infty$
$\sigma_G$	13.1.3	Geometrical Factors	0.21	R	$\sqrt{3}$	1	0.12	$\infty$
$\sigma_{CLV}$	13.1.9	Cleave Angle	0.015	R	$\sqrt{3}$	1	0.01	$\infty$
$\sigma_R$	13.1.4	Rotary Table	0.2	R	$\sqrt{3}$	1	0.12	$\infty$
$\sigma_\lambda$	13.1.5	Wavelength	0.08	N	1	1	0.08	$\infty$
$\sigma_T$	13.1.6	Temperature	0.01	N	1	1	0.01	$\infty$
$\sigma_{INT}$	13.1.7	Integration Routine	0.04	N	1	1	0.04	$\infty$
$\sigma_{REP}$	13.1.8	Reproducibility	0.136	N	1	1	0.136	>100
$\sigma_S$		Combined Uncertainty		N			0.309	>100
$U_{95}^S$		Expanded Uncertainty		N (k=2.0)			0.618	

Considering the more problematic alignment process of the fibre constrained within a zirconia ferrule an increase in the 'Geometrical Factors' uncertainty contribution from  $\pm 0.21\%$  to  $\pm 0.30\%$  was deemed reasonable although probably slightly pessimistic. This allowed for the slightly higher asymmetries and offsets encountered during the measurement process. The geometrical misalignment uncertainty contribution refers to such factors as the positioning of the fibre under measurement on the axis of rotation, vertical displacement of the detector fibre from optimum position and tilt or cleave angle of the fibre under measurement. The size of these effects were originally estimated by deliberately producing such misalignments and observing the consequent change in MFD. This subsequently increases the overall expanded uncertainty of measurement to  $\pm 0.666\%$  rounded to  $\pm 0.7\%$ .

The table 17 on the next page shows the modified uncertainties for these type of Qu grade patchcords.

**Table 17. Modified uncertainty budget for Qu grade patchcords**

Symbol	Para. Ref.	Source	Value $\pm$ %	Prob. Dist <sup>n</sup> .	Div.	c <sub>i</sub>	U <sub>i</sub> $\pm$ %	$\nu_i$
$\sigma_{LIN}$	13.1.2	System Linearity	0.32	R	$\sqrt{3}$	1	0.20	$\infty$
$\sigma_G$	13.1.3	Geometrical Factors	0.30	R	$\sqrt{3}$	1	0.17	$\infty$
$\sigma_{CLV}$	13.1.9	Cleave Angle	0.015	R	$\sqrt{3}$	1	0.01	$\infty$
$\sigma_R$	13.1.4	Rotary Table	0.2	R	$\sqrt{3}$	1	0.12	$\infty$
$\sigma_\lambda$	13.1.5	Wavelength	0.08	N	1	1	0.08	$\infty$
$\sigma_T$	13.1.6	Temperature	0.01	N	1	1	0.01	$\infty$
$\sigma_{INT}$	13.1.7	Integration Routine	0.04	N	1	1	0.04	$\infty$
$\sigma_{REP}$	13.1.8	Reproducibility	0.136	N	1	1	0.136	>100
$\sigma_S$		Combined Uncertainty		N			0.333	>100
$U_{95}^S$		Expanded Uncertainty		N (k=2.0)			0.666	

## 4.8 Summary

The Qu grade patchcord exhibited MFD values that agreed well with the commercial specification for the fibre type (G657.A1), however, it was clear that the mounting of the fibre within the ferrule created some compression of the bare fibre that showed as a flattening of the far-field intensity profile in the cladding mode regions at around  $\pm 15$  degs. This was not unexpected and importantly, did not ultimately affect the MFD values as the central region, containing the bulk of the propagated signal, dominates the integration. An apodizing effect, whereby pressure is applied to the fibre at the zirconia ferrule/cement region of the connector, could explain the small changes in the cross-sectional refractive index profile and the subsequent diffraction pattern. For this particular type of optical transmission, apodization involves modifying the shape of a mathematical function. Generally, in optics, it is primarily used to remove Airy disks caused by diffraction around an intensity peak, improving the focus. Non-circularities in the MFD were also at the levels expected from good quality optical fibre ranging from 0.08% to 0.23%. This is significant, as large non-circularities would be evidence that the build quality of the connectors would be insufficient for use within a Quantum internet, compromising its functional performance. Future work would allow for the removal of the connectors to measure the bare unconstrained fibre to assess more closely the contribution that the connectors play in affecting the MFD values and to calculate the effective area ( $A_{eff}$ ) using the far-field scan data. Ultimately, the measurements on this key parameter provide the manufacturer with confidence in their Quantum grade photonic components for commercialisation.

## 5 Concluding remarks and future collaborative opportunities.

It is worth noting that the flexibility of the systems described allows the characterisation of other key components necessary within a Quantum internet. The Insertion Loss system can accommodate other high-end components such as Quantum Photonic Integrated Circuits (QPIC's). Photonic Integrated Circuits (PICs) have seen extensive development over the past decade and are important components for the future of optical communications and optical metrology (eg: LIDAR and fibre-optic sensing applications) [6,7,8,9]. Even allowing for high initial costs and design complexities, the global Integrated Quantum Optical Circuits market is expected to reach \$1460.2 million by 2025 [10] with the increase in quantum computing driving the growth of the industry.

Quantum Photonic Integrated Circuits (QPICs or QuPICs) advance PIC technology to the quantum realm and allow for production and/or control of photonic quantum states for quantum applications. They are a compelling platform for extending quantum technologies to wider communication infrastructure - such as allowing for transfer of information in a distributed quantum computing environment. It is envisaged that QPICs will be an enabling technology for any sector where quantum information needs to be transferred or generated remotely, such as quantum encryption, quantum sensing and optical quantum computing. Measuring quantum efficiencies of QPIC's and their respective components using the pathway of a CHSH test platform (See Section 2 and Figures 2 - 4) would provide essential information to ensure successful operation at the quantum level.

As well as improving the traceable metrology aimed at entire QPIC/PIC interconnects such as insertion loss, polarization-dependent link/loss stabilities and return loss (including refined single, stepped and swept wavelength measurements), more specific metrology is based around structures and waveguides that perform specific functions. These include optical coupling [11], power splitting, wavelength division multiplexing or active elements affecting optical gain [12,13,14]. Accessing these structures to measure key parameters is technologically challenging and would require ongoing collaboration with manufacturers to develop PIC designs that allow access to key points and probing of test points along waveguide pathways.

Edge interfacing technologies can benefit from existing systems for characterizing optical intensity output profiles such as those used for mode field diameter that follow the far-field scanning method [15]. These include fibre tapering, used for fibre to PIC coupling [16] as well as endface waveguide modification utilizing such techniques as focused ion beam etching to modify and incorporate features into the end faces of optical fibre thereby altering far-field intensity profiles [30]. These links can be measured effectively by modifying systems and/or extending the operating ranges of measurements. Aligning optical connections and reducing mode-field mismatch is hugely important in the drive to minimize leakage/losses and more specifically, reducing decoherence of entangled photons and is currently a significant challenge to large scale fabrication [17,18,19]. These modified coupling techniques have far-reaching consequences for improved coupling efficiencies embracing interconnect boards [20,21] and maximising effective operating distances in quantum networks, as well as local operating efficiencies of PIC's and QPIC's. Understanding coupling

efficiencies for any quantum network is also complemented by other systems that can accommodate single-photon avalanche diodes (SPAD's) for low photon detection to characterise for detector efficiencies, dark count rates, after pulse probabilities and timing jitter. NPL has developed a system that can accommodate fibre coupled, as well as free space, single photon detectors. The integration of quantum grade interconnects within this system can be used to provide even more flexibility in assessing network efficiencies.

Longer-haul Quantum Grade links (G657A1/Hollow Core Fibre (HCF)) intended to connect are also able to be readily characterised on the systems in this report. Bend insensitive fibres such as G657.A1 are already available as quantum grade optical links for patchcords. Commercially available G657.A1 could benefit from more rigorous classical fibre metrology to reduce specified uncertainties. For example, a typical MFD value specified on a commercial fibre of this type is 9.3 – 10.3  $\mu\text{m}$  at 1550 nm and a dispersion coefficient of  $\leq 18$  ps/nm/km [22]. Quantum internet performance will require much more stringent knowledge of these parameters to maximise efficiencies and make use of primary systems such as those within NMI's.

Although HCF has been developed over approximately 30 years, only recently has its potential for longer haul communication systems been recognized. With very low losses ( $< 0.1$  dB/km at 1550 nm), low dispersion (3 ps/nm/km) and non-linearities and wide bandwidths, the future deployment for quantum applications is promising once it has become more cost effective to produce in significant lengths. Again, this technology would benefit from stringent characterizations of key parameters thereby providing industry confidence and accelerating adoption and subsequent deployment.

Several operators around the globe have been deploying HCF in their QKD systems. Following the first industrial deployment of a QKD network in the UK using standard fibre, recent demonstrations have claimed a world first with a trial of QKD over HCF [23] additional security is achieved using a Quantum Random Number Generator (QRNG). It is claimed that the test demonstrated that HCF is an excellent conduit for QKD transmission, enabling reduced latency and cutting down on interference between signals being transmitted over the fibre. This allowed QKD transmission to occur alongside other signals without impacting the security of the key transmission.

NPL and other NMI's capability, current expertise and future planning have shown that there is an urgent need to develop systems and measurement traceability for these interconnects [24]. Active involvement is needed in National and International standards bodies to harmonize the global approach towards standards thereby supporting industry and future research and development of this emerging technology. Significantly, the recent establishment of IEC committee JTC3 'Joint Technical Committee on Quantum Technologies' is an important development to coordinate and disseminate quantum interconnect standards activities. Work has also recently begun on a draft IEC standard 'Roadmap on Quantum Grade Interconnects' which will provide significant information as to the expected evolution of standards activity within this expanding field.

As has been demonstrated in this report, it is important to also recognize that existing standards can, in some cases, already provide, or accommodate quantum metrology requirements (existing standards for Mode Field Diameter, Polarization Mode Dispersion, Core-Cladding Concentricity, for example, are highly relevant to the requirements of quantum grade optical fibre and connectors). Insertion Loss and Return Loss (again already possessing established standards and protocols) can be further developed to accommodate Qu grade manufactured transmission links. Established expertise within leading NMI's, such as NPL, surrounding classical characterization of optical communication technologies can be used to extend existing or develop new traceable systems and knowledge. Quantum level metrology will not develop as an autonomous or solely independent technology but will be part of a marriage of classical and bespoke quantum systems that will significantly improve the quality and performance of new and emerging components and build confidence in developers and consumers alike in achieving the network efficiencies required for a practical Quantum internet.

## Appendix 1 – Example of a SENKO specification sheet for a quantum grade FC/UPC patchcord



**SENKO®**  
Advanced Components

# QUANTUM NETWORKING

**QU**




**BIT**

Unlike traditional computers, which use binary digits or bits to perform operations, quantum computers use quantum bits or qubits. Quantum computers are expected to be able to solve mathematical problems that cannot be solved using conventional computers. Although this problem-solving capability enables computation far beyond classical computing, it inevitably presents significant threats to cyber security & attack the foundations of today's cryptography. Quantum Key Distribution (QKD), a means of enabling secure encryption and authentication in the presence of the unbounded computational power to be introduced by quantum information technologies. QKD enables the exchange of secret symmetric keys used for encryption and authentication. These keys are secure, even against eavesdropping attempts powered by quantum computing. Senko is developing an optical approach to quantum computing with a line of Ultra Low-Loss connectors designed for Quantum Networking applications.

**FEATURES AND APPLICATIONS**

- Premium Super Low-Loss < 0.1dB
- Optical Return Loss > 80dB
- High Density
- Suitable for QKD Networks

**SN® /QuPC**  
CONNECTOR




4x Duplex  
in 1 Transceiver

**CS® /QuPC**  
CONNECTOR




Next Generation  
Duplex Connector

**LC /QuPC**  
CONNECTOR



Solid body  
Robust design

**SC /QuPC**  
CONNECTOR



Push-pull  
design



## References

- [1] A. Bahrami, A. Lord, and T. Spiller, "Quantum key distribution integration with optical dense wavelength division multiplexing: a review," *IET Quantum Commun.*, vol. 1, no. 1, pp. 9–15, 2020.
- [2] M. Lucamarini, Z. L. Yuan, J. F. Dynes, and A. J. Shields, "Overcoming the rate–distance limit of quantum key distribution without quantum repeaters," *Nature*, vol. 557, no. 7705, pp. 400–403, 2018.
- [3] Lee B, Pitwon R Jun 2020 White Paper QuPC® Connectors - Optical Interconnect for Quantum Networks.
- [4] Li J, Jia Q, Xue K, Wei DSL and Yu N 2022 A connection-oriented entanglement distribution design in quantum networks, *IEEE Transactions on Quantum Engineering*, 3, pp. 1-13, , Art no. 4100513, doi: 10.1109/TQE.2022.3176375.
- [5] IEE Proceedings - J, Vol 138 No.6 December 1991. "COST 217 Intercomparison and Analysis.
- [6] Hogan H, 2017 Senko, 2020 Data centre network: impact on optical interconnect & component technology *Photonics Spectra Lightwave Webcast* p36.
- [7] Ingham J D, Bamiedakis N, Penty RV, White IH., DeGroot JV and Clapp TV 2006 Multimode siloxane polymer waveguides for robust high-speed interconnects, *Conference on Lasers and Electro-Optics and 2006 Quantum Electronics and Laser Science Conference*.
- [8] Pitwon, R. 2016 Advances in photonic interconnect for data centre subsystems, Seagate Systems, UK, 4th Symposium on Optical Interconnect in Data Centres, ECOC 2016, Düsseldorf, Germany.
- [9] CIR., 2010. Board-level optical interconnects sales to hit \$5.6 billion by 2022 *Lightwave Staff article*
- [10] <https://www.alliedmarketresearch.com/integrated-quantum-optical-circuits-market> (accessed Sept 5th, 2022).
- [11] Selviah D et al 2017 Integrated optical and electronic interconnect PCB manufacturing research, *Circuit World* 36, 5–19.
- [12] IPC-TM-650, 1997. Test Methods Manual, The Institute for Interconnecting and Packaging Electronic Circuits Doc. No. 2.6.7, Rev. A.
- [13] IEC 61300-1:2016 - Fibre optic interconnecting devices and passive components – Basic test and measurement procedures – Part 1: General and guidance.
- [14] IEC 62496-2:2017 (E) - Optical circuit boards - Basic test and measurement procedures - Part 2:  
General guidance for definition of measurement conditions for optical characteristics of optical circuit boards.
- [15] IEC 60793-1-45 Measurement methods and test procedures — Mode field diameter.
- [16] Marchetti R, Lacava C, Carroll L, Gradkowski K, and Minzioni P 2019 Coupling strategies for silicon photonics integrated chips [Invited]," *Photon. Res.* 7, 201-239.
- [17] Eisenstein, M 2022 As pic production ramps up, fabricators eye alignment options *Photonics Spectra*.
- [18] Selviah DR, Fernandez FA, Papakonstantinou I, Wang K, Bagshiahi H, Walker AC, Mc-Carthy A, Suyal H, Hutt DA, Conway PP, Chappell J, Zakariyah SS and Milward D, 2008 Integrated optical and electronic interconnect printed circuit board manufacturing *Circuit World*, 34, pp. 21-26.
- [19] Bamiedakis N, Hashim A, Penty RV, White IH, 2012 Regenerative polymeric bus architecture for board-level optical interconnects *Optics Express* 20 11625 No. 11.

[20] CIR., 2010. Board-level optical interconnects sales to hit \$5.6 billion by 2022 Lightwave Staff article.

[21] Selviah D et al 2017 Integrated optical and electronic interconnect PCB manufacturing research, Circuit World 36, 5–19.

[22] <https://briticom.net/product/g657a1-fibre-optic-cable/>

[23] <https://www.fiercetelecom.com/tech/bt-eyes-quantum-security-boost-hollow-core-fiber-trial>

(accessed Jul. 14, 2022).

[24] NIST PML Photonics Priority: Metrology for advanced manufacturing <https://www.nist.gov/pml/pml-priority-photonics/pml-photonics-priority-metrology-advanced-manufacturing>.